Journal of Engineering Science and Technology
Vol. 15, No. 2 (2020) 1167 - 1185

MODELING AND SIMULATION OF POLLUTANTS DISPERSION IN NATURAL RIVERS USING COMSOL MULTIPHYSICS

NASSRIN J. AL-MANSORI, RASHA S. AL- KIZWINI, FATIMA K. AL- HUSSEINI*

Environmental Engineering Department,
College of Engineering, University of Babylon, 51001, Iraq
*Corresponding Author: fatimakarim437@gmail.com

Abstract

Two-dimensional mathematical model and COMSOL Multiphysics (version 5.3A) were used in the current study to model and simulate unsteady state continuous discharge of pollutants from multisource in the Shatt Al-Hilla River. To operate the model, the necessary information was experimentally measured, field measurements, from four wastewater outfalls and 13 stations along the studied reach of Shatt Al-Hilla River. The data were collected during the spring season, 15th April 2019, and winter season, 15th January 2019. The studied parameters, for water quality, were total dissolved solids (TDS), chloride (Cl^-), sulphate (SO_4), and biological oxygen demand (BOD). To check the reliability of the model, it was applied to two different sets of data collected on 15th February 2019 and 15th March 2019. Affectability examination was also performed to explore the impact of various factors on the outcomes anticipated by the application of the two-dimensional model. The standardization of a model shows that the perfect height of roughness is 0.025 m and the perfect slope of water is 7.5 cm/km. Additionally, McQuivey equation yielded perfect outcomes for standardization of the model. The results of the reliability check showed a good agreement between the experimental and the predicated data ($R^2 = 0.9$). Finally, both measured and predicated results indicated that Al-Farsi outfall is the most significant source of pollution, and it seriously influences the nature of the river water.

Keywords: Dispersion, Pollutant transport model, River pollution, Water quality.

1. Introduction

It is undeniable that the earth planet faces a serious environmental pollution crisis due to the activities of humankind [1-5]. Where the huge production of solid, liquid, and gaseous wastes have altered the natural ecosystem of the earth planet [6-9]. For instance, serious environmental problems, such as water crisis and climate changes, represent a direct threat to the existence of humankind [10-14].

Unfortunately, these problems are increasing due to several reasons, such as the increasing global population, and expansion in industrial activities [15-18]. One of the most significant problems is the water pollution due to the limited sources of fresh water, and due to its direct impact on human health [19-22]. Thus, several studies have been carried out either to track the pollution of freshwater resources or to develop treatment technologies, such as reverse osmosis, bio-remediation, and chemical treatments [23-25].

A significant part of these studies was devoted to developing a prediction or simulation models for a certain problem in the water resources, which helps engineers to prepare the required solutions for the potential problems. For instance, several studies were carried out to develop models that help to predict water quality at certain places, water quality administration, and movement of sediments [26, 27].

For example, Hashim et al. [28] developed a hydraulic model, depends basically on momentum and mass fraction conservation equations, to predict the relationship between the convection-diffusion and pollutants mass transport.

The outcomes of this model confirmed that the horizontal convection and diffusion predominant path in pollutants mass transport in the horizontal direction for pollutants with density ≤ 1000 kg/m^3. While for pollutants with density > 1000 kg/m^3, the predominant path in pollutants mass transport in the vertical direction is the vertical diffusion.

Al-Zboon and Al-Suhaili [29] developed a one-dimensional quality model to predict the variation in water quality in the Zarqa River. The studied parameters, as water quality parameters, were the biochemical oxygen demand (BOD), ammonium (NH_4), and dissolved oxygen (DO). Results of this study indicated high agreement between the measured and forecasted concentrations of the studied parameters.

Ramos-Fuertes et al. [30] constructed a model, based on field measurements, to predict the variation in water temperature in a mountainous reservoir and the Sil River (in Spain) due to discharging of the effluents of a hydroelectric plant.

In comparison with the results of the field measurements, the developed model showed good ability to simulate water temperature inside the river and the reservoir.

In this context, the current study aims to develop a model to forecast the pollutants transport along the Shatt Al-Hilla River. This study helps to determine the location of the critical pollution zones, which in turns helps engineers to select the right location for treatment facilities, capacity and type of treatment units, and to select the right location of irrigation intakes.

Objective of research

The current work aims to:

- Development of a two-dimensional model to simulate the pollutants transport along the Shatt Al-Hilla River. For this purpose, COMSOL Multiphysics software (version 5.3A) has been used as a tool to solve partial differential equations (PDE) and examine the common contact between river movement and concentrations of pollutants. Additionally, the *K*-*ε* turbulence model will be used to evaluate the horizontal and vertical speed profiles.
- Validate the applicability of the developed model to simulate the conditions of the Shatt Al-Hilla River by calculating the error percentage between the measured and predicated data.
- Specify the critical zones along the study reach, in which, the concentrations of pollutants exceed the allowable limits for irrigation water.

2. Forecasting of Aerodynamic Coefficients

The present work focuses on enduring continuous release of pollutants from different sources. To simplify the problem to a two-dimensional problem in a rectangular vertical plane, the following assumptions have been made [31]:

- The flow is uniform.
- The fluid is incompressible.
- The river reach is a rectangular vertical plane. The *x*-axis is along the water surface in the direction of flow, and the *z*-axis is along with the upstream downward.
- The slope of the river is very small, and the river surface is planar.
- Hydrostatic pressure is in a vertical direction.
- The river reach plane is constant across the river width.
- The pollutant is conservation, soluble or miscible substance having a density.
- Disregard the wind shear on the flow velocity.

2.1. Governing equations

The governing and auxiliary equations are:

2.1.1. *K*-*ε* turbulence model

The following equation represents the *K*-*ε* turbulence model [32]:

$$\mu_t = C_\mu \times \rho \times \frac{K^2}{\varepsilon} \tag{1}$$

where, μ_T: Eddy viscosity (kg^2/s^2), ρ: Fluid's density (kg/m^3), $C\mu$: Empirical constant represented by the dissipation coefficient in *K*-*ε* turbulence model, ε: Dissipation rate of turbulence kinetic energy per unit mass (m^2/s^3), *K*: Turbulence kinetic energy per unit mass (m^2/s^2) kinetic energy of turbulence defined as [32]:

$$\frac{1}{2}(u'^2 + v'^2 + w'^2) \tag{2}$$

where, u', v' and w' are fluctuating velocities in *x*, *y* and *z*-direction.

2.1.2. Advection-dispersion equation

Advection-dispersion phenomenon could be explained by Eq. (3) [32]:

$$\frac{\partial \bar{c}}{\partial t} + \bar{u}\frac{\partial \bar{c}}{\partial x} + \bar{v}\frac{\partial \bar{c}}{\partial y} + \bar{w}\frac{\partial \bar{c}}{\partial z} = E_x\frac{\partial^2 \bar{c}}{\partial x^2} + E_y\frac{\partial^2 \bar{c}}{\partial y^2} + E_z\frac{\partial^2 \bar{c}}{\partial z^2} \tag{3}$$

where, x: Longitudinal direction, y: Lateral direction and z: Vertical direction (L), u, v and w: Velocities in x, y and z directions, respectively (L/T), C: Concentration of substance, the function of x, y, z and time (M/L^3), t: Time (T), M: Self-diffusion coefficient (L^2/T), $E_x, E_y,$ and E_z : Turbulent diffusion coefficient in x, y, and z directions. Quantities with a symbol of "$^{-}$" are the mean values on an interval of time.

2.1.3. Dispersion coefficient equation

Fisher Eq. (4) [33]:

$$D_L = 0.011\frac{U^2T^2}{HU_*} \tag{4}$$

U: Stream velocity (m/s), D_L: Longitudinal dispersion coefficient (m^2/s), H: Cross-sectional average flow depth (m), U^*: Shear velocity (m/s), and T: Top width of water (m).

McQuivey and Keefer Eq. (5) [34]:

$$D_L = 0.058\left(\frac{Q}{ST}\right) \tag{5}$$

D_L: Longitudinal dispersion coefficient (m^2/s), Q: Discharge (m^3/s), S: Slope of bed channel (m/m), T: Top width of water (m).

Kashefipour Eq. (6) [35]:

$$D_L = 10.612\left(\frac{H}{U_*}\right)U^2 \tag{6}$$

2.1.4. Rough bed longitudinal speed spreading equation

The following formula is recommended to calculate the rough bed longitudinal speed spreading [35]:

$$U = 5.75\, U_* \log\left(\frac{30H}{K_s}\right) \tag{7}$$

U: Stream velocity (L/T), U^*: Shear velocity (L/T), H: Depth of flow (L), Ks: Roughness height (m).

3. Description of the Studied Reach

Shatt Al-Hilla River is one of the main water resources in the city of Babylon, Iraq. The total length of this river is about 95 km, its depth is between 4 and 5 m, and a width ranging from 40 to 100 m. The average side slope of this river is 1:3. Average glow velocity of Shatt Al-Hilla River is ranging between 0.25 to 0.45 m/s. To collect the required data for the development of the targeted model, a 4.5 km segment of the River was studied, as shown in Fig. 1. This segment includes four main wastewaters, namely Old Bridge, Gretaa, Al-Jamean, and Al-Farsi outfalls.

Additionally, 13 monitoring stations (*S*1-*S*13) were installed along this segment. Table 1 lists the details of these outfalls and monitoring stations.

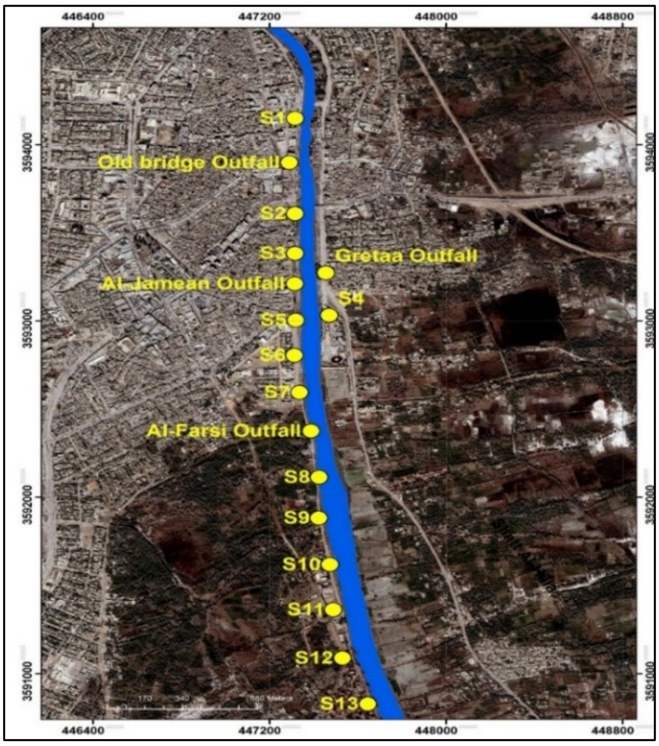

Fig. 1. The studied segment of the Shatt Al-Hilla River.

Table 1. Locations of the wastewater outfalls and monitoring stations.

Station no.	Distance (km)	Coordinates
***S*1**	0.00	447344E, 3594258N
Old bridge outfall	0.300	447276E, 3593924N
***S*2**	0.588	447325E, 3593652N
***S*3**	0.876	447322E, 3593524N
At Gretaa outfall	0.878	447417E, 3593343N
***S*4**	1.078	447440E, 3592431N
Al-Jamean outfall	0.880	447338E, 3593198N
***S*5**	1.080	447317E, 3593004N
***S*6**	1.280	447312E, 3592805N
***S*7**	1.480	447334E, 3592595N
Al-Farsi outfall	1.500	447386E, 3592376N
***S*8**	2.000	447424E, 3592114N
***S*9**	2.500	447422E, 3591966N
***S*10**	3.000	447472E, 3591619N
***S*11**	3.500	447553E, 3591100N
***S*12**	4.000	447726E, 3590611N
***S*13**	4.500	448018E, 3590188N

Sampling and laboratory test

The experimental work, in this research, has been divided into two parts: field and laboratory work. Where the fieldwork concerned collection of samples from Shatt Al-Hilla River. Sampling process has been carried out using a 5 m wooden rode that supplied with a 2 L plastic container. Samples were collected from the middle of the river, then transported into polyethylene containers and stored according to the standard preservation methods for each test. For example, for the BOD test, the collected water samples were placed in a dark container at 20 ^{0}C, then these containers were placed in a cool box and immediately sent to the laboratory.

Laboratory works concerned the accurate measurement of the targeted pollutants, which included chloride (Cl), sulphates (SO_4), total dissolved solid (TDS), and BOD. These measurements were carried out in the Laboratories of the Department of Environmental Engineering at the University of Babylon. Table 2 summarises the testing methods, tools, and materials.

Table 2. Summary of testing methods, tools, and materials.

Parameter	Name of method or device	Used materials
Total dissolved solid (TDS)	Lovibond device HM digital (COM-100)	-
Chloride (Cl)	Argent metric method by titration against Silver nitrate	• Silver nitrates • Binary potassium chromates (dye) • Burette • Pipette
Sulphates (SO_4)	Gravimetric method with ignition of residue	• Diluted hydrochloric acid (0.1 N) • Barium chloride Nomination papers (ashless) • Heter • Eyelid • Burning furnace • Sensitive balance
Biological oxygen demand (BOD)	Lovibond device (LS-1601678)	• Nitrification • Potassium hydroxide

4. Results and Discussion

Based on the guideline for surface water, the maximum permissible concentration of TDS is 1500 mg/L [36]. According to the obtained data from the experimental work, Fig. 2, the measured concentrations of the TDS at all monitoring stations and wastewater outfalls were within the allowable limits, except measured values at Al-Farsi outfall where the concentration of TDS exceeded 1600 mg/L. These results indicate the significant impact of this outfall on the water quality of the river, which could be attributed to the lack of treatment to the wastewater that discharged at this point.

The maximum allowable chloride concentration in natural water is limited to 200 mg/L [37]. According to Fig. 3, only two stations (*S*7 and *S*13) have met the recommended limits for chloride concentration in surface water. This high concentration of chloride could be attributed to the chemical composition of the bed of the river because it has been reported that soil of this river is chloride-rich one [38]. The same trend has been noticed in the measured concentrations of sulphates, where all the studied stations and wastewater outfalls showed elevated concentrations of sulphate except *S*7, Fig. 4. The main reason for these elevated concentrations is the sulphate naturally occur in the soil of the studied river [38]. It is noteworthy to highlight that the measured concentrations of both sulphate and chloride in the water Shatt Al-Hilla River significantly increased during the wet season. This increase in the concentrations of sulphate and chloride could be explained by the washing of these pollutants from the neighbour areas to the river (due to the rain).

Finally, the measured BOD concentrations are shown in Fig. 5. It can be noticed from this figure that the measured concentrations of BOD at all monitoring stations were within the allowable limits (5 mg/L), however, it was significantly higher than allowable limits for surface water at the wastewater outlets. Where measured concentrations of BOD, during the winter season, at old bridge outfall, Gretaa outfall, Al-Jamean outfall, and Al-Farsi outfall were about 110, 89, 104, and 118 mg/L, respectively. While during the summer season, the measured concentrations of BOD at old bridge outfall, Gretaa outfall, Al-Jamean outfall, and Al-Farsi outfall were about 78, 79, 102, and 101 mg/L, respectively.

According to these results, the average concentration of BOD at the wastewater outfalls were about 20 times and 18 times higher than the allowable limit during winter and summer seasons, respectively. These values are significantly high in comparison with the measured concentrations of BOD in the other parts of the River, which means that the passage of the effluent wastewater through the treatment plants in Hilla city did not seem to significantly enhance the removal of biochemical oxygen demanding substances from the effluent wastewater before they discharged to the river course. In fact, these results indicate the inefficiency of the treatment plants in Hilla city in removing biochemical oxygen demanding substances from wastewater. According to the results of Figs. 2 to 4, the critical zones could be considered at the wastewater outfalls.

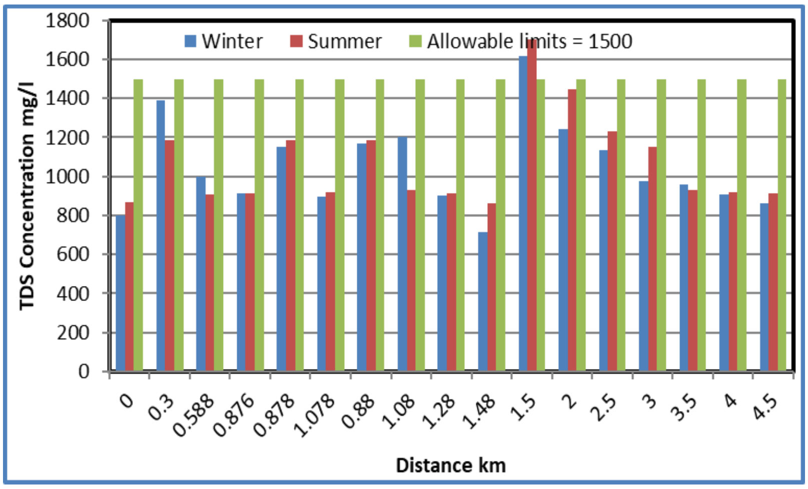

Fig. 2. Variation of TDS concentrations with distance during the studied period.

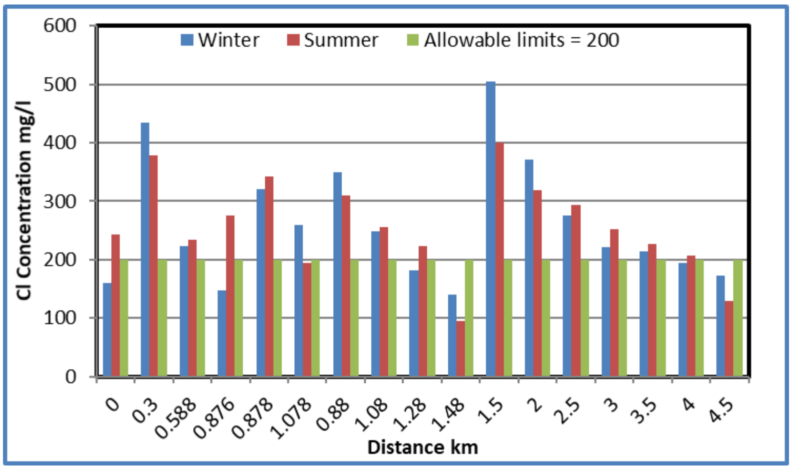

Fig. 3. Variation of Cl concentrations with distance during the studied period.

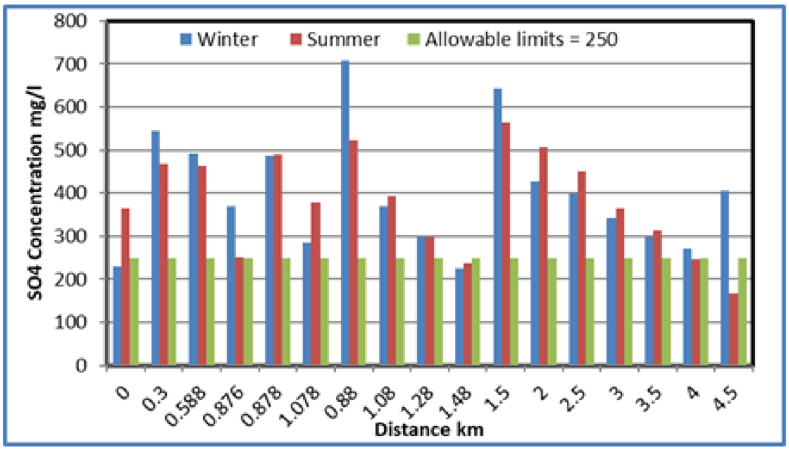

Fig. 4. Variation of SO_4 concentrations with distance during the studied period.

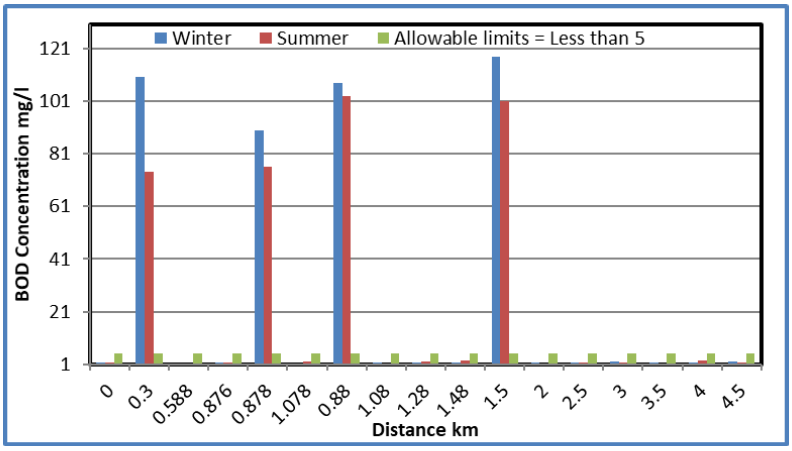

Fig. 5. Variation of BOD concentrations with distance during the studied period.

5. Model Development

5.1. Model calibration

The two-dimensional numerical model is based on a strong coupling between the *k-ε* turbulent model and advection-dispersion equation to simulate hydrodynamic parameters that govern the pollutants transport along the studied segment. The first comparison was in term of roughness height (*Ks*). The influence of three different values of *Ks* (0.012 m, 0.025 m, 0.036 m) on the dispersion of the studied pollutants (TDS, chloride, sulphate and BOD) were examined.

Figure 6 shows a comparison between the forecasted and measured concentrations along the studied segment during the period from 15th January to 15th March 2019. Two important facts can be noticed from this figure; firstly, increasing the roughness height increases the dispersion of pollutants as it causes an increase in water mixing and a decrease in velocity of the water. Secondly, this figure indicates a good agreement between the forecasted and measured values, which proves the applicability of the developed model for Shatt Al-Hilla River.

A second comparison has been made in terms of the slope of the riverbed (*S*). Three values were tested in the present model, which are 6 cm/km, 7.5 cm/km and 9 cm/km to show the comparison between the observed and predicted values of TDS, Cl-, SO_4^{-2} and BOD concentration along the study reach measured on 15th January to 15th March 2019. Figure 7 shows that any increase in the water slope will cause a decrease in the concentrations of TDS, Cl-, SO_4^{-2}, which could be attributed to the increase in the velocity of the river and vice versa. From Fig. 7, it can be concluded that the best correlation coefficient is obtained at water slope of 7.5 cm/km.

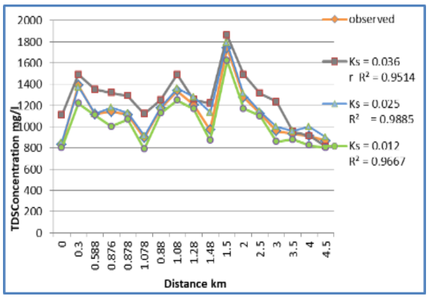

(a) For TDS.

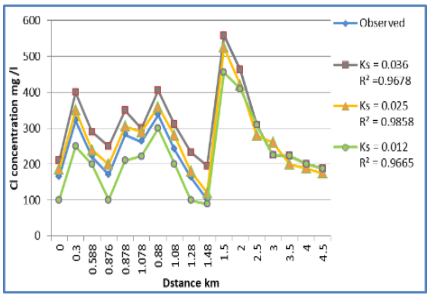

(b) For Cl-.

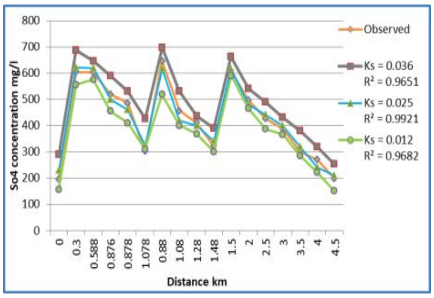

(c) For SO4.

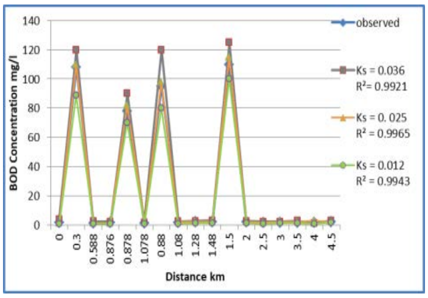

(d) For BOD.

Fig. 6. Calibration of the model at different values of *Ks*.

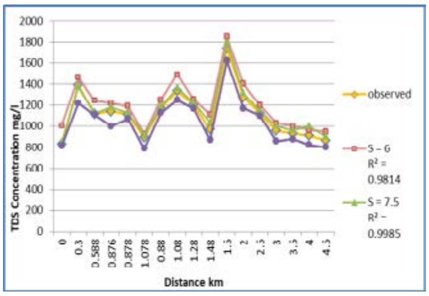

(a) For TDS.

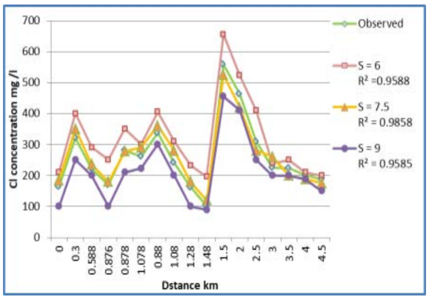

(b) For Cl$^-$.

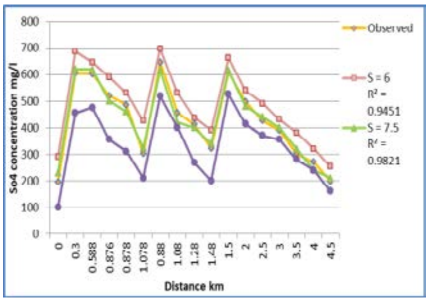

(c) For SO_4.

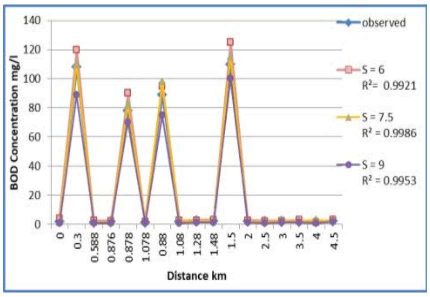

(d) For BOD.

Fig. 7. Calibration of the model at different values of *S*.

The final comparison was in term of the Longitudinal Dispersion coefficient (D_L) as shown in Fig. 8. In this comparison, three equations were used; namely Fischer Eq., McQuivey Eq., and Kashefipour and Falconer equation to calculate the longitudinal dispersion coefficient (D_L).

The comparison between the predicated and measured concentrations of the studied pollutants (TDS, chloride, sulphate, and BOD). It can be observed from this figure that the McQuivey equation gives the nearest outcomes to the experimental ones.

Comparisons in terms of *Ks*, *S*, and D_L were repeated for a set of data that collected on the 15th of March 2019. The results of these comparisons are shown in Figs. 9 to 11.

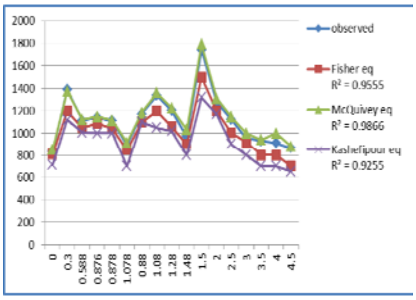

(a) For TDS.

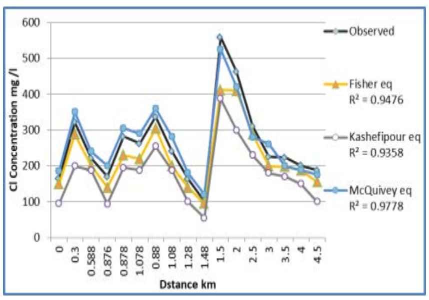

(b) For Cl$^-$.

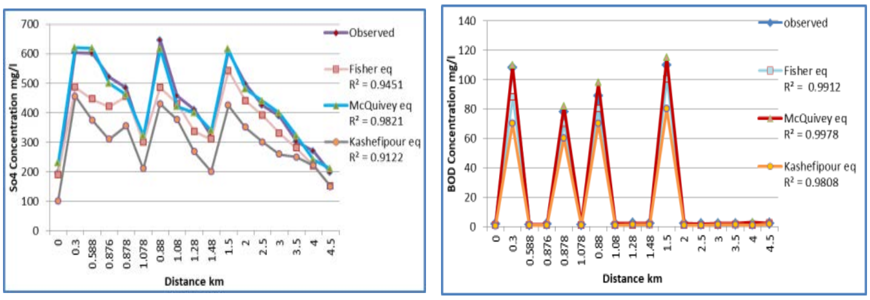

(c) For SO_4. **(d) For BOD.**

Fig. 8. Calibration of the model at different values of D_L.

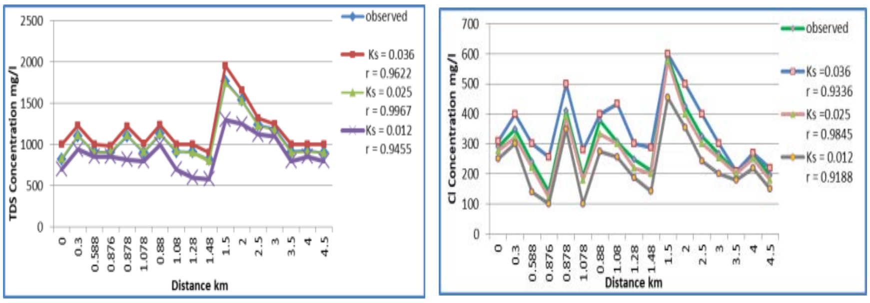

(a) For TDS. **(b) For Cl.**

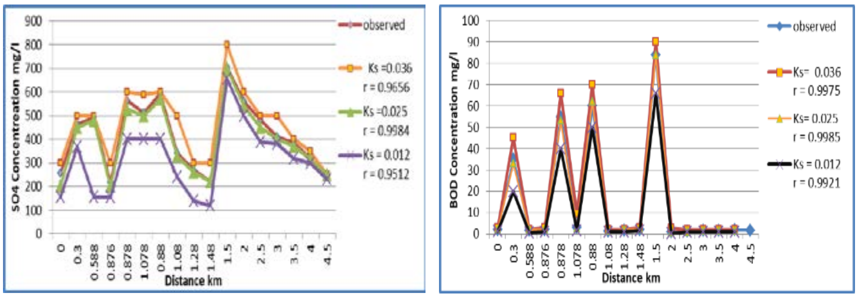

(c) For SO_4. **(d) For BOD.**

Fig. 9. Calibration of the model at different values *Ks*.

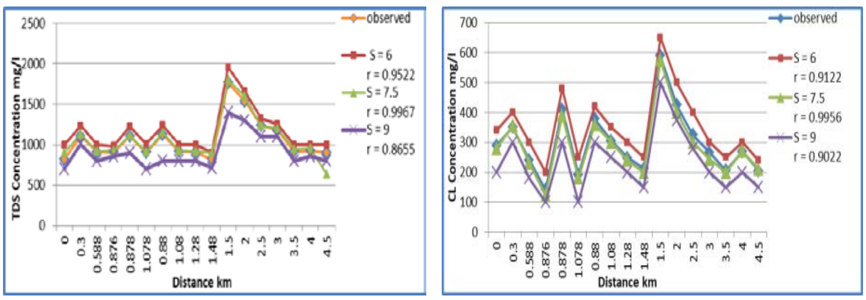

(a) For TDS. **(b) For Cl^{-1} .**

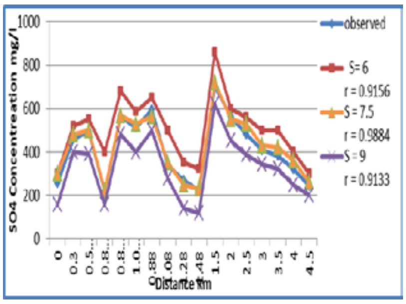

(c) For SO_4.

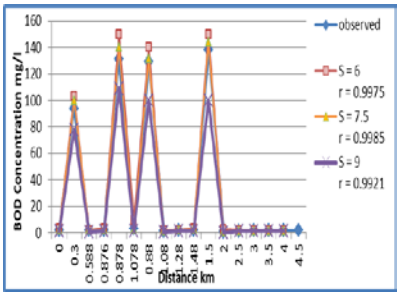

(d) For BOD.

Fig. 10. Calibration of the model at different values *S*.

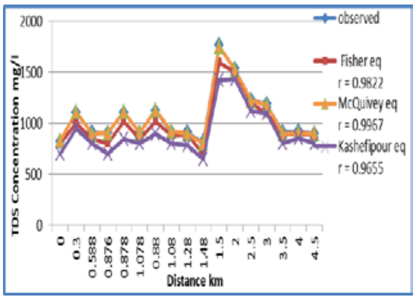

(a) For TDS.

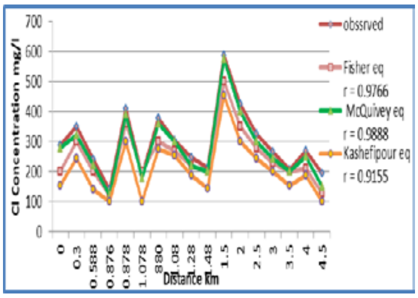

(b) For Cl^-.

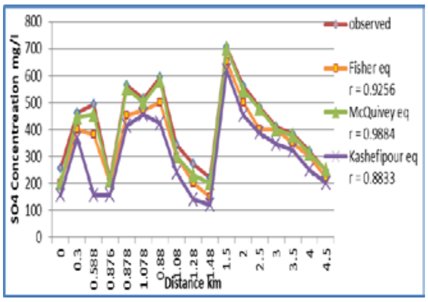

(c) For SO_4.

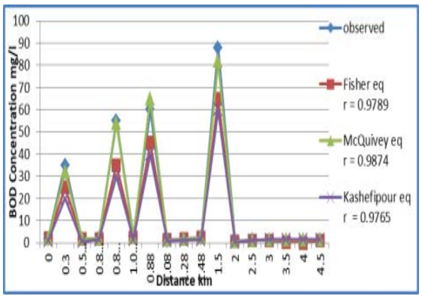

(d) For BOD.

Fig. 11. Calibration of the model at different values D_L.

5.2. Validation of the model

In this phase of the study, the used values of roughness height and slope of the bed were 0.025 m 7.5 cm/km, respectively (from the previous phase of the study). Longitudinal dispersion coefficient (D_L) and lateral dispersion coefficient (D_T) were assessed using McQuivey and Fischer equations separately. The forecasted concentrations of different pollutants, including TDS, chloride, sulphate, and BOD were compared with the measured values on the 15th of February 2019, and on the 15th of April 2019. Tables 3 to 6 list the outcomes of these comparisons. The obtained results indicate a good agreement between measured and predicated concentrations with a percentage error of less than 10% that indicate the applicability of the developed model to forecast the pollutants transport along Shatt Al-Hilla River. In comparison with the results of previous works, the obtained trend from the current study is similar to that obtained by Al-Zboon and Al-Suhaili [29] and Ramos-Fuertes et al. [30]. Finally, the recent development in the sensing methods [39-41] could be used to monitor the dispersion of pollutants in rivers, which will provide valuable real-time data about the behaviour of the targeted data.

Table 3. Comparison between measured and forecasted concentrations of TDS, Cl^-, and SO_4 on the 15th of February 2019.

Distance	TDS			Cl^-			SO_4		
(km)	*M*	*F*	*E%*	*M*	*F*	*E%*	*M*	*F*	*E%*
0.00	155	155	0	155	155	0	262	262	0
0.300	550.8	570	3.49	550	570	3.49	489	490	0.20
0.588	225	210	7.14	225	210	7.14	380	350	8.57
0.876	125	120	4.17	125	120	4.17	220	215	2.33
0.878	405	400	1.25	405	400	1.25	493	500	1.42
1.078	214	215	0.46	214	215	0.46	271	270	0.37
0.880	361	350	3.14	361	350	3.14	772	280	2.94
1.080	256	250	2.4	256	250	2.4	282	280	0.71
1.280	201	200	0.5	201	200	0.5	182	180	1.11
1.480	179	180	0.56	179	180	0.56	130	130	0
1.5	450	465	3.33	450	465	3.33	680	678	0.42
2.00	280	280	0	280	280	0	431	430	0.23
2.5	241	250	3.73	241	250	3.73	301	310	2.99
3.00	220	225	2.27	220	225	2.27	298	300	0.67
3.5	205	200	2.5	205	200	2.5	292	295	1.03
4.00	190	200	5.3	190	200	5.3	271	280	3.32
4.5	158	130	5.3	158	130	5.3	208	200	4.00

M = measured, *F* = forecasted, *E*% = error

Table 4. Comparison between measured and forecasted concentrations of BOD on the 15th of February 2019.

Distance (km)	Measured BOD	Forecasted BOD	Error %
0.00	1.8	1.8	0
0.300	113	115	1.77
0.588	1	1	0
0.876	1.6	1.54	3.89
0.878	103	110	6.79
1.078	1.5	1.45	3.45
0.880	128	130	4.84
1.080	1.2	1.15	4.35
1.280	1.3	1.25	4
1.480	1.6	1.55	3.23
1.5	126	130	3.17
2.00	1.4	1.36	2.94
2.5	2	2	0
3.00	2.2	2.15	2.33
3.5	1.7	1.6	6.25
4.00	1.5	1.4	7.14
4.5	1.7	1.6	6.25

Table 5. Comparison between measured and forecasted concentrations of TDS, Cl^-, and SO_4 on the 15th of April 2019.

Distance (km)	TDS			Cl^-			SO_4		
	M	***F***	***E%***	***M***	***F***	***E%***	***M***	***F***	***E%***
0.00	915	915	0	298	298	0	273	273	0
0.300	1263	1300	2.93	398	435	9.29	575	583	1.39
0.588	908	950	4.63	248	266	7.25	435	450	3.44
0.876	922	980	6.29	411	444	8.02	288	296	2.77
0.878	1264	1300	2.85	374	385	2.94	617	622	0.81
1.078	932	1000	7.29	198	213	7.57	446	453	1.56
0.880	1247	1280	2.65	290	311	7.24	651	644	1.08
1.080	941	1000	6.26	305	320	4.91	246	240	2.5
1.280	917	970	5.78	248	250	0.80	164	155	5.80
1.480	904	950	5.09	78	82	5.12	82	80	2.5
1.5	1640	1600	2.5	511	532	4.10	625	612	2.12
2.00	1353	1370	1.25	411	420	2.18	452	450	4.44
2.5	1222	1250	2.29	362	371	2.48	422	435	3.08
3.00	1120	1150	2.67	288	300	4.16	320	333	4.06
3.5	942	1000	6.16	248	255	2.82	246	251	2.03
4.00	913	975	6.79	245	250	2.04	172	130	6.17
4.5	933	950	1.82	106	114	7.54	90	90	0

M = measured, *F* = forecasted, *E*% = error

Table 6. Comparison between measured and forecasted concentrations of BOD on the 15th of April 2019.

Distance (km)	Measured BOD	Forecasted BOD	Error%
0.00	1.8	1.8	0
0.300	114	120	5.26
0.588	1.35	1.41	3.70
0.876	1.7	1.6	6.25
0.878	103	110	6.79
1.078	1.4	1.45	3.57
0.880	118	120	1.69
1.080	1.2	1.2	0
1.280	2.2	2.18	0.92
1.480	2.6	2.5	4.00
1.5	122	120	1.67
2.00	1.5	1.46	2.74
2.5	1.4	1.4	0
3.00	2.1	2	5.00
3.5	1.8	1.82	1.11
4.00	1.1	1.08	1.85
4.5	2.9	2.87	1.04

6. Conclusions

Generally, the following conclusions could be drawn from conducting the present work:

- The water quality assessment of the river as shown in results above indicated that the measured TDS concentrations are generally within the allowable limits (except at Al-Farsi outfall). However, the obtained results indicated that the River is polluted with SO_4 and Cl (measured concentrations are more the allowable limits in all monitoring stations and wastewater outfalls). In terms of BOD, the measured concentrations are exceeded the allowable limits only at wastewater outfalls.
- Measured and forecasted concentrations of the studied pollutants, at the critical zones, exceeded the Iraqi river maintenance standards. Thus, the river water is not recommended, at these zones, for irrigation and drinking purposes.
- The developed model is sensitive to both roughness height and bed slope.
- McQuivey equation provides nearest outcomes to the experimental measurements.
- The distribution of pollutants increases with the decrease in the bed slope due to the decrease in velocity of the water. Additionally, the distribution of pollutants increases with the increase of roughness height for the same reason.

Nomenclatures

C	Concentration, mg/L
$\bar{c}$	Time-averaged concentration, mg/l
D_L	Coefficient of dispersion, m^2/s
E_x	Turbulent diffusion coefficient in the *x*-direction, cm^2/s
E_y	Turbulent diffusion coefficient in the *y*-direction, cm^2/s
K	Turbulence kinetic energy per unit mass, m^2/s^2
K_s	Roughness height, m
M	Self-diffusion coefficient (L^2/T)
Q	Discharge, m^3/s
R	Hydraulic radius, m
S	Slope
T	Top width of water, m
t	Time, s
U	Stream velocity, m/s
$\bar{u}$	Time-averaged velocity in the *x*-direction, m/s
$\bar{v}$	Time-averaged velocity in the *y*-direction, m/s
$\bar{w}$	Time-averaged velocity in the *z*-direction, m/s

Greek Symbols

ε	Dissipation rate of turbulence kinetic energy
μ	Dynamic fluid viscosity, m^2/s
μ_T	Eddy viscosity, m^2/s
$C\mu$	Empirical constant represented
ρ	Fluid's density kg/m^3
σ_ε	Turbulent Prandtl numbers for the dissipation rate

Abbreviations

BOD	Biological Oxygen Demand
CFD	Computational fluid dynamics
PDE	Partial Differential Equation
TDS	Total Dissolved Solid

References

1. Goudie, A.S. (2018). *The human impact on the natural environment* (8th ed.). Hoboken, New Jersey, United States of America: Wiley Blackwell.
2. Hashim, K.S.; Al Khaddar, R.; Jasim, N.; Shaw, A.; Phipps, D.; Kot, P.; Pedrola, M.O.; Alattabi, A.W.; Abdulredha, M.; and Alawsh, R. (2018). Electrocoagulation as a green technology for phosphate removal from river water. *Separation and Purification Technology*, 210, 135-144.
3. Al-Saati, N.H.; Hussein, T.K.; Abbas, M.H.; Hashim, K.; Al-Saati, Z.N.; Kot, P.; Sadique, M.; Aljefery, M.H.; and Carnacina, I. (2019). Statistical modelling of turbidity removal applied to non-toxic natural coagulants in water treatment: A case study. *Desalination and Water Treatment*, 150, 406-412.
4. Hashim, K.S.; Idowu, I.A.; Jasim, N.; Al Khaddar, R.; Shaw, A.; Phipps, D.; Kot, P.; Pedrola, M.O.; Alattabi, A.W.; Abdulredha, M.; Alawsh, R.; Teng, K.H.; Joshi, K.H.; and AlJefery, M.H. (2018). Removal of phosphate from River water using a new baffle plates electrochemical reactor. *MethodsX*, 5, 1413-1418.
5. Hashim, K.S.; Shaw, A.; Al Khaddar, R.; Pedrola, M.O.; and Phipps, D. (2017). Defluoridation of drinking water using a new flow column-electrocoagulation reactor (FCER) - experimental, statistical, and economic approach. *Journal of Environmental Management*, 197, 80-88.
6. Abdulredha, M.; Al Khaddar, R.; Jordan, D.; Kot, P.; Abdulridha, A.; and Hashim, K. (2018). Estimating solid waste generation by hospitality industry during major festivals: A quantification model based on multiple regression. *Waste Management*, 77, 388-400.
7. Abdulredha, M.; Al Khaddar, R.; Jordan, D.; and Hashim, K. (2017). The development of a waste management system in Kerbala during major pilgrimage events: Determination of solid waste composition. *Procedia Engineering*, 196, 779-784.
8. Idowu, I.A.; Atherton, W.; Hashim, K.; Kot, P.; Alkhaddar, R.; Alo, B.I.; and Shaw, A. (2019). An analyses of the status of landfill classification systems in developing countries: Sub Saharan Africa landfill experiences. *Waste Management*, 87, 761-771.
9. Al-Jumeily, D.; Hashim, K.; Alkaddar, R.; Al-Tufaily, M.; and Lunn, J. (2018). Sustainable and environmental friendly ancient reed houses (inspired by the past to motivate the future). *Proceeedings of the 11th International Conference on Developments in eSystems Engineering*. Cambridge, United Kingdom, 214-219.
10. Paterson, M.; and Stripple, J. (2016). Singing climate change into existence: on the territorialization of climate policymaking. *The Social Construction of Climate Change*, 7, 24 pages.

11. Zubaidi, S.L.; Al-Bugharbee, H.; Muhsen, Y.R.; Hashim, K.; Alkhaddar, R.M.; Al-Jumeily, D.; and Aljaaf, A.J. (2020). A prediction of municipal water demand: Case study in Iraq. *Proceedings of the 12th International Conference on Developments in eSystems Engineering (DeSE)*. Kazan, Russia, 25-32.
12. Zubaidi, S.L.; Kot, P.; Hashim, K.; Alkhaddar, R.; Abdellatif, M.; and Muhsin, Y.R. (2019). Using LARS-WG model for prediction of temperature in Columbia City, USA. *Proceedings of the International Conference on Civil and Environmental Engineering Technologies*. Najaf, Iraq, 9 pages.
13. Hashim, K.S.; Shaw, A.; Al Khaddar, R.; Pedrola, M.O.; and Phipps, D. (2017). Energy efficient electrocoagulation using a new flow column reactor to remove nitrate from drinking water - Experimental, statistical, and economic approach. *Journal of Environmental Management*, 196, 224-233.
14. Hashim, K.S.; Al-Saati, N.H.; Hussein, A.H.; and Al-Saati, Z.N. (2018). An investigation into the level of heavy metals leaching from Canal-Dreged Sediment: A case study metals leaching from dreged sediment. *Proceedings of the International Conference on Materials Engineering and Science*. Istanbul, Turkey, 12-22.
15. Hashim, K.S.; Shaw, A.; Al Khaddar, R.; Pedrola, M.O.; and Phipps, D. (2017). Iron removal, energy consumption and operating cost of electrocoagulation of drinking water using a new flow column reactor. *Journal of Environmental Management,* 189, 98-108.
16. Shubbar, A.A.; Jafer, H.; Dulaimi, A.; Hashim, K.; Atherton, W.; and Sadique, M. (2018). The development of a low carbon binder produced from the ternary blending of cement, ground granulated blast furnace slag and high calcium fly ash: An experimental and statistical approach. *Construction and Building Materials,* 187, 1051-1060.
17. Shubbar, A.A.; Al-Shaer, A.; AlKizwini, R.S.; Hashim, K.; Al Hawesah, H.; and Sadique, M. (2019). Investigating the influence of cement replacement by high volume of GGBS and PFA on the mechanical performance of cement mortar. *Proceedings of the International Conference on Civil and Environmental Engineering Technologies*. Najaf, Iraq, 31-38.
18. Hashim, K.S.; Ali, S.S.M.; AlRifaie, J.K.; Kot, P.; Shaw, A.; Al Khaddar, R.; Idowu, I.; and Gkantou, M. (2020). Escherichia coli inactivation using a hybrid ultrasonic–electrocoagulation reactor. *Chemosphere*, 247, 125868.
19. Khan, S.; Shahnaz, M.; Jehan, N.; Rehman, S.; Shah, M.T.; and Din, I. (2013). Drinking water quality and human health risk in Charsadda district, Pakistan. *Journal of Cleaner Production*, 60, 93-101.
20. Abdulhadi, B.A.; Kot, P.; Hashim, K.S.; Shaw, A.; and Khaddar, R.A. (2019). Influence of current density and electrodes spacing on reactive red 120 dye removal from dyed water using electrocoagulation/electroflotation (EC/EF) process. *Proceedings of the International Conference on Civil and Environmental Engineering Technologies*. Najaf, Iraq, 7 pages.
21. Hashim, K.S.; Al-Saati, N.H.; Alquzweeni, S.S.; Zubaidi, S.L.; Kot, P.; Kraidi, L.; Hussein, A.H.; Alkhaddar, R.; Shaw, A.; and Alwash, R. (2019). Decolourization of dye solutions by electrocoagulation: An investigation of the effect of operational parameters. *Proceedings of the International Conference on Civil and Environmental Engineering Technologies*. Najaf, Iraq, 8 pages.

22. Hashim, K.S.; AlKhaddar, R.; Shaw, A.; Kot, P.; Al-Jumeily, D.; Alwash, R.; and Aljefery, M.H. (2020). Electrocoagulation as an eco-friendly river water treatment method. *Advances in Water Resources Engineering and Management*, 219-235.
23. Crini, G.; and Lichtfouse, E. (2019). Advantages and disadvantages of techniques used for wastewater treatment. *Environmental Chemistry Letters*, 17(1), 145-155.
24. Alattabi, A.W.; Harris, C.; Alkhaddar, R.; Alzeyadi, A.; and Hashim, K. (2017). Treatment of residential complexes' wastewater using environmentally friendly technology. *Procedia Engineering*, 196, 792-799.
25. Alattabi, A.W.; Harris, C.B.; Alkhaddar, R.M.; Hashim, K.S.; Ortoneda-Pedrola, M.; and Phipps, D. (2017). Improving sludge settleability by introducing an innovative, two-stage settling sequencing batch reactor. *Journal of Water Process Engineering*, 20, 207-216.
26. Fu, B.; Merritt, W.S.; Croke, B.F.; Weber, T.; and Jakeman, A.J. (2018). A review of catchment-scale water quality and erosion models and a synthesis of future prospects. *Environmental modelling and software*, 114, 75-97.
27. Kannan, N.; Santhi, C.; White, M.J.; Mehan, S.; Arnold, J.G.; and Gassman, P.W. (2019). Some challenges in hydrologic model calibration for large-scale studies: A case study of SWAT model application to Mississippi-Atchafalaya river basin. *Hydrology*, 6(1), 23 pages.
28. Hashim, K.S.; Kot, P., Zubaidi, S.L.; Alwash, R.; Al Khaddar, R.; Shaw, A.; Al-Jumeily, D.; and Aljefery, M.H. (2020). Energy efficient electrocoagulation using baffle-plates electrodes for efficient Escherichia coli removal from wastewater. *Journal of Water Process Engineering*, 33, 1-7.
29. Al-Zboon, K.K.; and Al-Suhaili, R.H. (2009). Improvement of water quality in a highly polluted river in Jordan. *Jordan Journal of Civil Engineering*, 3(3), 283-293.
30. Ramos-Fuertes, A.; Palau, A.; and Dolz, J. (2018). Application of a two-dimensional water quality model (CE-QUAL-W2) to the thermal impact assessment of a pumped-storage hydropower plant project in a mountainous reservoir (Matalavilla, Sil River, Spain). *Advances in Hydroinformatics*, 301-314.
31. Al-Zubaidy, H.A.M. (2007). *A two dimensional numerical model for simulation of the dispersion of pollutants in Shatt Al-Hilla*. Master Thesis. College of Engineering, University of Babylon, Babylon, Iraq.
32. Markatos, N.C. (1986). The mathematical modelling of turbulent flows. *Applied Mathematical Modelling*, 10(3), 190-220.
33. Fischer, H.B.; List, J.E.; Koh, R.C.Y.; Imberger, J.; and Brooks, N.H. (1979). *Mixing in inland and coastal waters*. San Diego, California, United States of America: Academic Press, Inc.
34. McQuivey, R.S.; and Keefer, T.N. (1974). Simple method for predicting dispersion in streams. *Journal of the Environmental Engineering Division*, 100(4), 997-1011.
35. Kashefipour, S.M.; and Falconer, R.A. (2002). Longitudinal dispersion coefficients in natural channels. *Water Research*, 36(6), 1596-1608.

36. Abbasnia, A.; Yousefi, N.; Mahvi, A.H.; Nabizadeh, R.; Radfard, M.; Yousefi, M.; and Alimohammadi, M. (2019). Evaluation of groundwater quality using water quality index and its suitability for assessing water for drinking and irrigation purposes: Case study of Sistan and Baluchistan province (Iran). *Human and Ecological Risk Assessment: An International Journal*, 25(4), 988-1005.
37. Phoonsawat, K.; Ratnarathorn, N.; Henry, C.S.; and Dungchai, W. (2018). A distance-based paper sensor for the determination of chloride ions using silver nanoparticles. *Analyst*, 143(16), 3867-3873.
38. Manea, M.H.; Al-Tawash, B.S.; and Al-Saady, Y.I. (2019). Hydrochemical characteristics and evaluation of surface water of Shatt Al-Hilla, Babil Governorate, Central Iraq. *Iraqi Journal of Science*, 60(3), 583-600.
39. Teng, K.H.; Kot, P.; Muradov, M.; Shaw, A.; Hashim, K.; Gkantou, M.; and Al-Shamma'a, A. (2019). Embedded smart antenna for non-destructive testing and evaluation (NDT&E) of moisture content and deterioration in concrete. *Sensors*, 19(3), 12 pages.
40. Ryecroft, S.P.; Shaw, A.; Fergus, P.; Kot, P.; Hashim, K.; Conway, L.; and Moody, A. (2020). A novel gesomin detection method based on microwave spectroscopy. *Proceedings of the 12th International Conference on Developments in eSystems Engineering (DeSE)*. Kazan, Russia, 5 pages.
41. Ryecroft, S.; Shaw, A.; Fergus, P.; Kot, P.; Hashim, K.; Moody, A.; and Conway, L. (2019). A first implementation of underwater communications in raw water using the 433 MHz frequency combined with a bowtie antenna. *Sensors*, 19(8), 10 pages.